RAPID COMMUNICATIONS

PHYSICAL REVIEW E **72**, 020601(R) (2005)

Renormalization group approach to multiscale simulation of polycrystalline materials using the phase field crystal model

Nigel Goldenfeld
Department of Physics, University of Illinois at Urbana-Champaign, 1110 West Green Street, Urbana, Illinois 61801-3080, USA

Badrinarayan P. Athreya and Jonathan A. Dantzig
Department of Mechanical and Industrial Engineering, University of Illinois at Urbana-Champaign 1206 West Green Street, Urbana, Illinois 61801, USA

(Received 6 January 2005; revised manuscript received 14 June 2005; published 18 August 2005)

We propose a computationally efficient approach to multiscale simulation of polycrystalline materials, based on the phase field crystal model. The order parameter describing the density profile at the nanoscale is reconstructed from its slowly varying amplitude and phase, which satisfy rotationally covariant equations derivable from the renormalization group. We validate the approach using the example of two-dimensional grain nucleation and growth.

DOI: 10.1103/PhysRevE.72.020601 PACS number(s): 81.15.Aa, 81.16.Rf, 05.10.Cc, 61.72.Cc

Why is it so hard to predict the properties of real materials? Unlike simple crystalline solids, real materials, produced by a wide range of processing conditions, contain defects and multiple grains that strongly impact mechanical, thermal, and electrical responses, and give rise to such important phenomena as plasticity, hysteresis, work hardening, and glassy relaxation. Moreover, it is frequently the case that a faithful description of materials processing requires simultaneous treatment of dynamics at scales ranging from the nanoscale up to the macroscopic. For example, dendritic growth, the generic mode of solidification of most metals and alloys, involves the capillary length at the nanoscale, the emergent pattern dimensions on the scale of microns, and the thermal or particle diffusion length on the scale of 10^{-4} m, in addition to the grain and sample size.

Despite these obstacles, progress in rational material design requires a fundamental understanding of the way in which useful properties emerge as the mesoscale is approached. Questions that must be addressed include: What is the collective behavior of assemblies of nanoscale objects? How best to achieve target mesoscale properties from nanoscale constituents? And how can the properties at the nano-, meso-, and intermediate scales simultaneously be captured quantitatively and predictively?

A number of computational approaches to handle the range of length scales have been proposed recently [1,2], including quasi-continuum methods [3–6], the heterogeneous multiscale method [7,8], multiscale molecular dynamics [9–12], multigrid variants [13], and extensions of the phase field model [14]. These techniques strive to provide a unified description of the many scales being resolved, but in some cases require nonsystematic ways to link the disparate scales to enable treatment of sufficiently large mesoscale systems. This can introduce spurious modes and excitations, and difficulties associated with the transition between scales [2,8]. Most of this work is limited to crystalline materials with a few isolated defects [15].

In this paper, we propose a theoretical approach to these difficulties, by combining the phase field crystal (PFC) formalism [16,17] with the renormalization group (RG) [18,19] and related methods (see, e.g., [20]), developed for the analysis of hydrodynamic instabilities in spatiallyextended dynamical systems [21–28]. We present effective equations at the mesoscale, from which the atomic density can readily be reconstructed, and show that this approach is capable of generating high fidelity representations of materials processing dynamics. Moreover, we demonstrate that the mesoscale equations—analogs of rotationally covariant amplitude and phase equations in fluid convection [29]—are computationally tractable and amenable in future work to adaptive grid techniques.

Our approach is based on a form of the RG that unifies the singular perturbation theory [21], and is a fully systematic way to extract universal or large-scale structures from spatially extended dynamical systems. The basic idea is to start, not with a molecular dynamics model at the nanoscale, but with a density functional description (in this context, the phase field crystal model), whose equilibrium solutions are periodic density modulations. A system that is periodic at the nanoscale can be parametrized in terms of a uniform phase and an amplitude: the amplitude describes the maximum variations in the density of the system through the unit cell, while the phase describes uniform spatial translations. A system with underlying periodicity, but which also contains defects or other nanostructures, can be represented by a density wave whose amplitude is at most slowly varying on the nanoscale, and a phase that is essentially uniform everywhere, except near a defect. This observation suggests that the phase of the density is the appropriate dynamical variable to use for describing spatially modulated nanoscale structure in a mesoscopic system, and in the vicinity of a defect it must be supplemented by the amplitude.

For any spatially extended pattern-forming dynamics, RG provides a prescription for obtaining slowly varying amplitudes and phase equations valid on scales much larger than the nanoscale [21–25]. These equations possess the key advantage that their solutions are essentially uniform, with localized rapid variations near defects. The renormalization procedure used here is more general than real-space renormalization, which has been attempted in related contexts [9,12]. In particular, our technique directly focuses on the instabilities that characterize the dynamics, which may not have simple real-space interpretations. Once the amplitude and phase are determined, the actual structure at the nanoscale (and above) can be reconstructed. Because the amplitude and phase equations describe solutions that are slowly varying everywhere, except near a defect, adaptive mesh refinement can be used to solve the amplitude and phase equations.

Phase field crystal model. The phase field crystal model is a continuum, nonlinear partial differential equation for the density $\rho(\vec{x})$ that recently has been shown [16,17] to capture realistic aspects of materials dynamics, including grain growth, ductile fracture, epitaxial growth, solidification processes, and reconstructive phase transitions. In addition, the model natively supports elasticity theory, both linear and nonlinear, without any *ad hoc* modeling. Thus, the PFC can address the important problem of nanoscale strain effects, and their coupling from the nanoscale to the continuum.

Let $F\{\rho\}$ denote the coarse-grained free energy functional whose minima correspond to the equilibrium (lattice) state of a d-dimensional system, and whose corresponding chemical potential gradient drives the dynamics of ρ. A simple form of F that gives rise to a triangular lattice equilibrium state is the Brazovskii form [30],

$$F\{\rho(\mathbf{x})\} = \int d^d\vec{x}\{\rho[\alpha\Delta T + \lambda(q_o^2 + \nabla^2)^2]\rho/2 + u\rho^4/4\}, \quad (1)$$

where α, λ, q_o, and u can be related to material properties [16,17], and ΔT denotes the temperature difference from some (higher) reference temperature. It is convenient to rewrite this free energy in dimensionless units, i.e., $\vec{x} \equiv \vec{r}q_o, \psi \equiv \rho\sqrt{u/\lambda q_o^4}, r \equiv a\Delta T/\lambda q_o^4, \tau \equiv \Gamma\lambda q_o^6 t$, where Γ is a phenomenological constant [17], and $F \rightarrow Fu/\lambda^2 q_o^{8-d}$ so that the equation of continuity for the density becomes

$$\partial\psi/\partial t = \nabla^2([r + (1 + \nabla^2)^2]\psi + \psi^3) + \zeta. \quad (2)$$

The conserved Gaussian noise will not generally be important for describing phase transition kinetics, and so will henceforth be neglected here.

The mean-field phase diagram of the PFC equation (2) can be calculated analytically [17] in a one-mode approximation that is valid in the limit of small r, and represented in the plane of dimensionless temperature, r, and dimensionless average density, $\bar{\psi}$. Three possible equilibrium solutions exist: a "liquid," $\psi_C = \bar{\psi}$; a two-dimensional "crystal" with triangular symmetry, $\psi_T = A_T[\cos(q_T x)\cos(q_T y/\sqrt{3}) - \cos(2q_T y/\sqrt{3})/2] + \bar{\psi}$; and a smectic phase that will be ignored for the present purposes. The triangular lattice can exhibit persistent defect structures during the relaxation to equilibrium.

Key to differentiating our approach from others is the fact that the PFC method was designed to investigate phenomena on diffusive time scales that are typically many orders of magnitude longer than the time scales accessible in molecular dynamics simulations. On the other hand, the PFC method suffers from some of the same drawbacks as molecular dynamics simulation: by resolving the nanoscale, brute force computation on a massive scale is required to capture mesoscale phenomena. We finesse this difficulty here by working with the slowly varying amplitude and phase description.

Mesoscale representation of the PFC. The dynamics of the slowly varying amplitude and phase describes fluctuations about a given set of lattice vectors, but must be covariant with respect to rotations of those lattice vectors, in order to properly describe polycrystalline materials with arbitrarily oriented grains. A similar situation arises in describing amplitude and phase variations of convection rolls, and in the context of the model Swift-Hohenberg [31] equations, the form of the governing equations was originally proposed by Gunaratne *et al.* [32], and derived systematically from the RG formalism of Chen *et al.* [21] by Graham [22] (see also Ref. [23]).

The triangular phase solution is represented as

$$\psi(\vec{x}) = \sum_j A_j(t)\exp(i\vec{k}_j \cdot \vec{x}) + \bar{\psi}, \quad (3)$$

where $\vec{k}_1 = k_0(-\vec{i}\sqrt{3}/2 - \vec{j}/2), \vec{k}_2 = k_0\vec{j}$ and $\vec{k}_3 = k_0(\vec{\mathrm{i}}\sqrt{3}/2 - \vec{\mathrm{j}}/2)$ are the reciprocal lattice vectors, k_0 is the wave number of the pattern, $\vec{i}$ and $\vec{j}$ are unit vectors in the x and y directions, and A_j $(j=1,2,3)$ are the complex amplitude functions. The detailed derivation of the evolution equations for the RG form of the PFC equation, similar to the approaches referenced above, will be given elsewhere. We simply present the result here due to space limitations

$$\frac{\partial A_1}{\partial t} = \tilde{\mathcal{L}}_1 A - 3A_1(|A_1|^2 + 2|A_2|^2 + 2|A_3|^2) - 6\bar{\psi}A_2^* A_3^* \quad (4)$$

(together with appropriate permutations for A_2 and A_3), where

$$\tilde{\mathcal{L}}_j = [1 - \vec{\nabla}^2 - 2i\vec{k}_j \cdot \vec{\nabla}][-r - 3\bar{\psi}^2 - \{\vec{\nabla}^2 + 2i\vec{k}_j \cdot \vec{\nabla}\}^2] \quad (5)$$

is the manifestly rotationally covariant operator. After solving the RG equations in Eq. (4), the density is reconstructed using Eq. (3).

Model Validation. For ease of numerical implementation, we have chosen to solve the amplitude equations about a globally fixed basis of lattice vectors. As a result, the grain orientation information must be borne by the complex amplitude functions A_j. We specify this information through an initial condition $A_j(\theta)$, where θ is the rotation angle measured with respect to the basis vectors, and the function $A_j(\theta)$ is chosen such that, when the original field ψ is reconstructed as per Eq. (3), the resulting grain is rotated by an angle θ.

Figure 1 shows the time evolution for the nucleation and growth of a two-dimensional film as predicted by the RG equation, starting from an initial condition of randomly oriented seeds, with $\bar{\psi}=0.285$ and $r=-0.25$. The initial crystallite domains grow, colliding to form a polycrystalline microstructure. The solutions obtained using the PFC equation are essentially indistinguishable from Fig. 1, indicating excellent

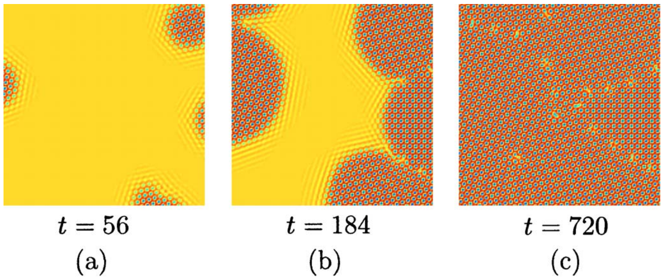

FIG. 1. (Color online) RG-reconstructed density at indicated times for heterogeneous nucleation and growth in a two-dimensional film.

qualitative agreement. The key feature of the RG equation is its ability to correctly capture defect formation and motion.

As a more rigorous demonstration of accuracy, Fig. 2 compares the grain-boundary energy, γ, as a function of the misorientation angle θ, predicted using the two algorithms. The initial condition for this test comprised two misaligned crystals separated by a narrow strip of liquid, on a periodic domain (see [17] for details). Figure 2 also shows the Read-Shockley equation [33], a well-known analytical result for small angle grain boundaries, that has been scaled to fit large misorientation data. The agreement is particularly good for low angle grain boundaries, and the values predicted by the RG equations closely follow the trends predicted by the PFC (from [17]) and the Read-Shockley equation. The maximum difference in the free energy as computed by the RG and PFC equations is about 1.6%.

Computational efficiency. Figure 3 (inset) shows the grid convergence behavior in the Read-Shockley test of the solutions to the PFC and RG equations. The crystals are misoriented by the maximum possible angle, $\pi/6$. We define the error $\varepsilon_0 = |\|y^{\Delta x}\|_2 - \|y^0\|_2|$, where $\|y^{\Delta x}\|_2$ is the L_2 norm of the solution for a mesh spacing of Δx, and $\|y^0\|_2$ is the L_2 norm obtained by Richardson extrapolation to $\Delta x = 0$ consistent with a second-order finite difference method. For a comparable level of accuracy, we see that $\Delta x_{RG} \approx 2\Delta x_{PFC}$. In a forward Euler time step scheme, this leads to a stability condition $\Delta t_{RG} \approx 6\Delta t_{PFC}$. Clearly, the RG equations offer significant opportunities for improved computational efficiency.

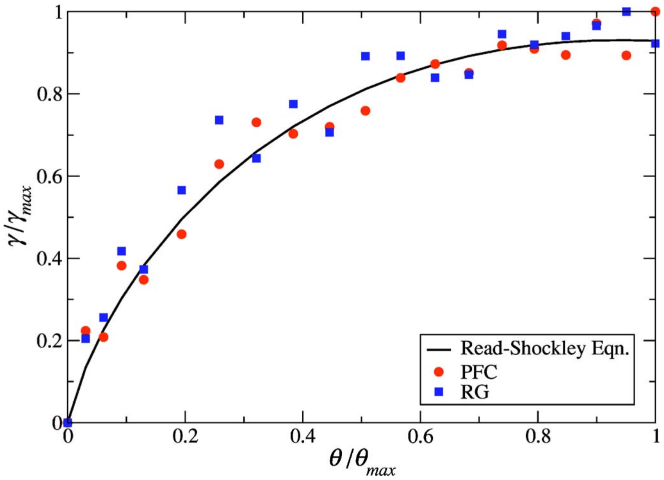

FIG. 2. (Color online) Comparison of grain-boundary energy predicted by the RG and PFC equations, with the Read-Shockley equation.

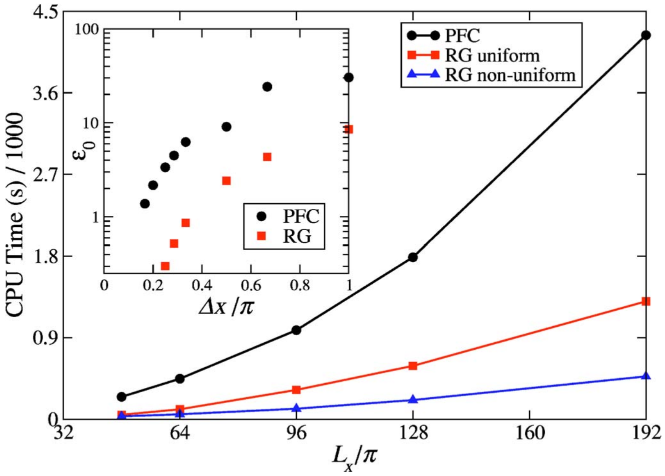

FIG. 3. (Color online) Scaling of CPU time vs domain length L_x for the PFC and RG equations. The inset shows the error in the respective solutions with diminishing mesh spacing Δx.

Figure 3 compares the CPU time as a function of domain size L_x for the Read-Shockley test with $\Delta\theta = 3.88°, r = -0.25$, and $\bar{\psi} = 0.28$, showing that the CPU time required for the RG equations ranges from about 5 to 6 times less than for the PFC equations. Consistent with the grid convergence behavior described above, we chose $\Delta x_{PFC} = \pi/4$, $\Delta t_{PFC} = 0.008$, $\Delta x_{RG} = \pi/2$, $\Delta x_{RG} = \pi/2$ and $\Delta t_{RG} = 0.05$. The difference in the free energy predicted by the RG equations and PFC equations was $<0.1\%$. Even more significantly, however, the amplitude functions can be solved on a nonuniform computational grid. For this problem, since the location of the boundary is known *a priori*, it is easy to construct an appropriate nonuniform mesh. We chose constant $\Delta y = \pi/2$, and allowed Δx to vary from a minimum of $\pi/2$ to 2π. This reduced the size of the computational mesh from 257×257 to 97×257. Even with this relatively naive implementation, we find that the speedup of the RG form compared to the original PFC form is close to a factor of 10 (see Fig. 3), while the error in the free energy is still $<0.1\%$. We anticipate the computational benefits of solving these equations on a fully adaptive mesh to be much higher.

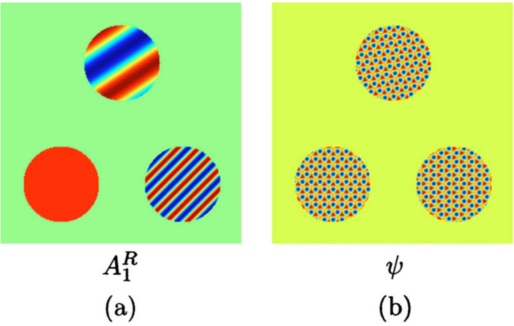

FIG. 4. (Color online) (a) Real component of the complex amplitude; (b) density field ψ reconstructed using Eq. (3). Clockwise from the lower left: $\theta = 0, \pi/24$, and $\pi/6$.

One limitation to the approach described here is that the orientation information causes a spatial variation in the amplitude when it is represented using the basis vectors of the triangular lattice. This is illustrated in Fig. 4, showing the real part of one of the complex amplitude functions, and the corresponding reconstructed density variable ψ for three different orientations. The "beats" evident in Fig. 4(a), which contain grain orientation information, persist as the grains evolve. This phenomenon could limit the effectiveness of adaptive mesh methods, since the mesh has to resolve these structures. We note, however, that if we write the complex amplitudes as $A_j = \Psi_j \exp(i\Phi_j)$, where Ψ_j is the amplitude modulus and Φ_j is the phase angle, we can formulate equations of motion for Ψ_j and $\nabla\Phi_j$ from Eq. (4), fields that are uniform everywhere (no beats) except near defects and interfaces. The resulting adaptive grid algorithm can thus be made to scale much more optimally [34], with interface or grain-boundary length rather than the area of significantly misoriented grains. We will present this work in a future article.

In summary, we have shown that multiscale modeling of complex polycrystalline materials microstructure is possible using a combination of continuum modeling at the nanoscale using the PFC model, RG, and related techniques from spatially extended dynamical systems theory. Our equations are well suited for efficient adaptive mesh refinement, thus enabling realistic modeling of large-scale materials processing and behavior.

This work was supported in part by the National Science Foundation through Grant No. NSF-DMR-01-21695 and by the National Aeronautics and Space Administration through Grant No. NAG8-1657. We thank Professor Ken Elder for several useful discussions.

---

[1] R. Phillips, *Crystals, Defects and Microstructures: Modeling Across Scales* (Cambridge University Press, Cambridge 2001).

[2] D. D. Vvedensky, J. Phys.: Condens. Matter **16**, R1537 (2004).

[3] E. B. Tadmor, M. Ortiz, and R. Phillips, Philos. Mag. A **73**, 1529 (1996).

[4] V. B. Shenoy, R. Miller, E. B. Tadmor, R. Phillips, and M. Ortiz, Phys. Rev. Lett. **80**, 742 (1998).

[5] J. Knap and M. Ortiz, J. Mech. Phys. Solids **49**, 1899 (2001).

[6] R. E. Miller and E. B. Tadmor, J. Comput.-Aided Mater. Des. **9**, 203 (2002).

[7] W. E, B. Enquist, and Z. Huang, Phys. Rev. B **67**, 092101 (2003).

[8] W. E and Z. Huang, Phys. Rev. Lett. **87**, 135501 (2001).

[9] R. E. Rudd and J. Q. Broughton, Phys. Rev. B **58**, R5893 (1998).

[10] J. Q. Broughton, F. F. Abraham, N. Bernstein, and E. Kaxiras, Phys. Rev. B **60**, 2391 (1998).

[11] C. Denniston and M. O. Robbins, Phys. Rev. E **69**, 021505 (2004).

[12] S. Curtarolo and G. Ceder, Phys. Rev. Lett. **88**, 255504 (2002).

[13] J. Fish and W. Chen, Comput. Methods Appl. Mech. Eng. **193**, 1693 (2004).

[14] J. A. Warren, R. Kobayashi, A. E. Lobkovsky, and W. C. Carter, Acta Mater. **51**, 6035 (2003).

[15] W. E and X. Li (unpublished), http://www.math.princeton.edu/multiscale/el.ps

[16] K. R. Elder, M. Katakowski, M. Haataja, and M. Grant, Phys. Rev. Lett. **88**, 245701 (2002).

[17] K. R. Elder and M. Grant, Phys. Rev. E **70**, 051605 (2004).

[18] N. Goldenfeld, O. Martin, Y. Oono, and F. Liu, Phys. Rev. Lett. **64**, 1361 (1990).

[19] N. Goldenfeld, *Lectures on Phase Transitions and the Renormalization Group* (Addison-Wesley, Reading, MA, 1992).

[20] C. Bowman and A. C. Newell, Rev. Mod. Phys. **70**, 289 (1998).

[21] L. Y. Chen, N. Goldenfeld, and Y. Oono, Phys. Rev. E **54**, 376 (1996).

[22] R. Graham, Phys. Rev. Lett. **76**, 2185 (1996).

[23] K. Nozaki, Y. Oono, and Y. Shiwa, Phys. Rev. E **62**, R4501 (2000).

[24] S. Sasa, Physica D **108**, 45 (1997).

[25] Y. Shiwa, Phys. Rev. E **63**, 016119 (2000).

[26] M. C. Cross and A. C. Newell, Physica D **10**, 299 (1984).

[27] T. Passot and A. C. Newell, Physica D **74**, 301 (1994).

[28] A. C. Newell, T. Passot, and J. Lega, Annu. Rev. Fluid Mech. **25**, 399 (1993).

[29] M. C. Cross and P. C. Hohenberg, Rev. Mod. Phys. **65**, 851 (1993).

[30] S. A. Brazovskii, Zh. Eksp. Teor. Fiz. **68**, 175 (1975).

[31] J. Swift and P. C. Hohenberg, Phys. Rev. A **15**, 319 (1977).

[32] G. H. Gunaratne, Q. Ouyang, and H. Swinney, Phys. Rev. E **50**, 2802 (1994).

[33] W. T. Read and W. Shockley, Phys. Rev. **78**, 275 (1950).

[34] N. Provatas, N. Goldenfeld, and J. Dantzig, Phys. Rev. Lett. **80**, 3308 (1998).